

Co-precipitation of MnO and Cu in an ionic liquid as a first step toward self-formed barrier layers

Paul-Henri Haumesser¹, Catherine C. Santini², Laurence Massin³, and Jean-Luc Rousset³

¹Univ. Grenoble Alpes, F-38000 Grenoble, France ; CEA, LETI, MINATEC Campus, F-38054 Grenoble, France.

²Univ. Lyon, CNRS-UMR 5265, 43 Bd du 11 Novembre 1918, F-69616, Villeurbanne Cedex, France.

³Univ. Lyon, IRCELYON, UMR 5256, CNRS, Villeurbanne, France

1 Monitoring the decomposition of Mn(^tBuCH₂)₂ in IL

The reactivity of Mn(^tBuCH₂)₂ ($5 \times 10^{-2} \text{ mol} \cdot \text{L}^{-1}$) in solution in C₁C₄ImNTf₂ (4 mL) was studied in a 100 mL autoclave connected to a continuous flow reactor under H₂ (0.4 MPa) at 100 °C. The gas phase was continuously analysed by gas chromatography. After 24 h, the equivalent of 8.5 C per Mn (i.e. 1.7 (^tBuCH₂) ligand out of 2 per Mn atom) had evolved as alkanes (mainly methane C₁, ethane C₂, neopentane C₅ and propane C₃).

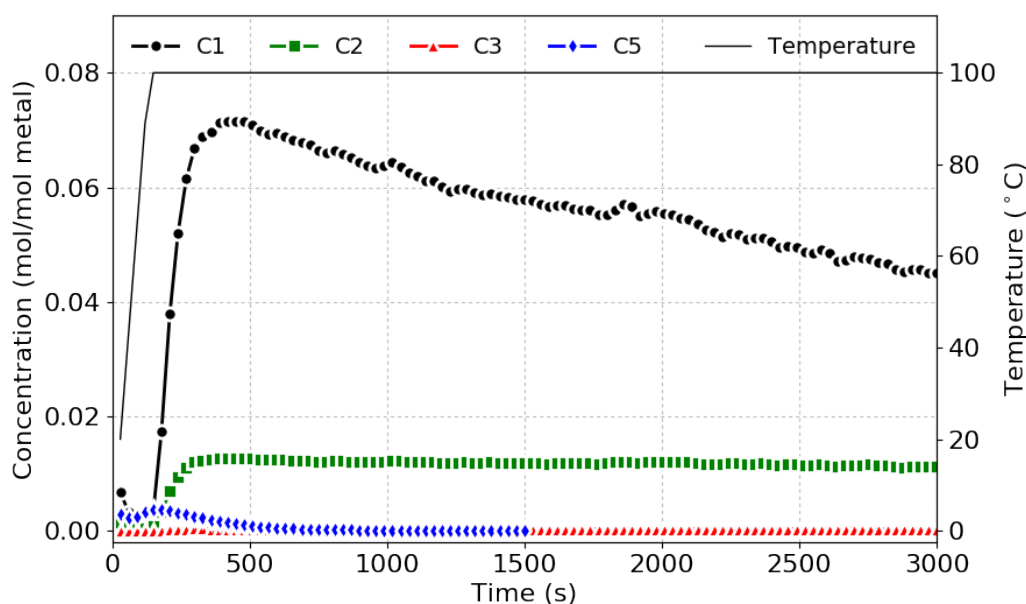


Figure S11: Time evolution as measured by gas chromatography of decomposition products of Mn(^tBuCH₂)₂ in C₁C₄ImNTf₂ under H₂ at 100 °C.

2 EDX and HRTEM characterisation of NPs formed by decomposing $\text{Mn}(\text{}^t\text{BuCH}_2)_2$

The EDX spectrum of a nanoparticle obtained after decomposition of $\text{Mn}(\text{}^t\text{BuCH}_2)_2$ under 0.9 MPa H_2 at 50 °C for 48 h in $\text{C}_1\text{C}_4\text{ImNTf}_2$ is plotted in Figure SI2. As expected, Mn is detected. Please note the presence of Cu on this spectrum, which arises from the column rather than from the sample. Also, some Mg is detected, probably due to a residual contamination in the Mn precursor.

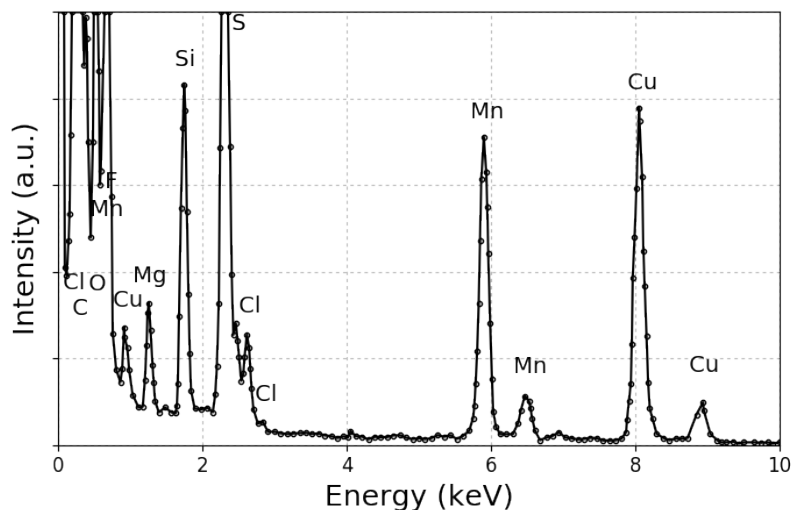


Figure SI2: EDX response of a nanoparticle obtained after decomposition of $\text{Mn}(\text{}^t\text{BuCH}_2)_2$ under 0.9 MPa H_2 at 50 °C for 48 h in $\text{C}_1\text{C}_4\text{ImNTf}_2$.

A typical HRTEM picture of one of the NPs produced by decomposing $\text{Mn}(\text{}^t\text{BuCH}_2)_2$ is displayed in Figure SI3a. The presence of Mn in the NP is confirmed by EDX (Figure SI2). The Fourier transform of the HRTEM image forms a regular pattern that could be indexed using various structures, including cubic and tetragonal lattices. The cubic structure in Figure SI3b corresponds to β -Mn, while the second cubic lattice in Figure SI3c is compatible with either α -Mn or MnO. Finally, the tetragonal phase in Figure SI3d compares with that of Mn_3O_4 .

Table SI1: Comparison between measured and computed interplanar distances of the NP in Figure SI3.

#	Exp. Å	β -Mn		α -Mn		Tetragonal	
		hkl	Å	hkl	Å	hkl	Å
1	1.65	-213	1.68	4-23	1.65	-1-33	1.64
2	2.81	-201	2.82	3-10	2.81	0-13	2.78
3	2.50	-21-1	2.57	20-3	2.47	113	2.53
4	2.74	01-2	2.82	-11-3	2.68	120	2.73

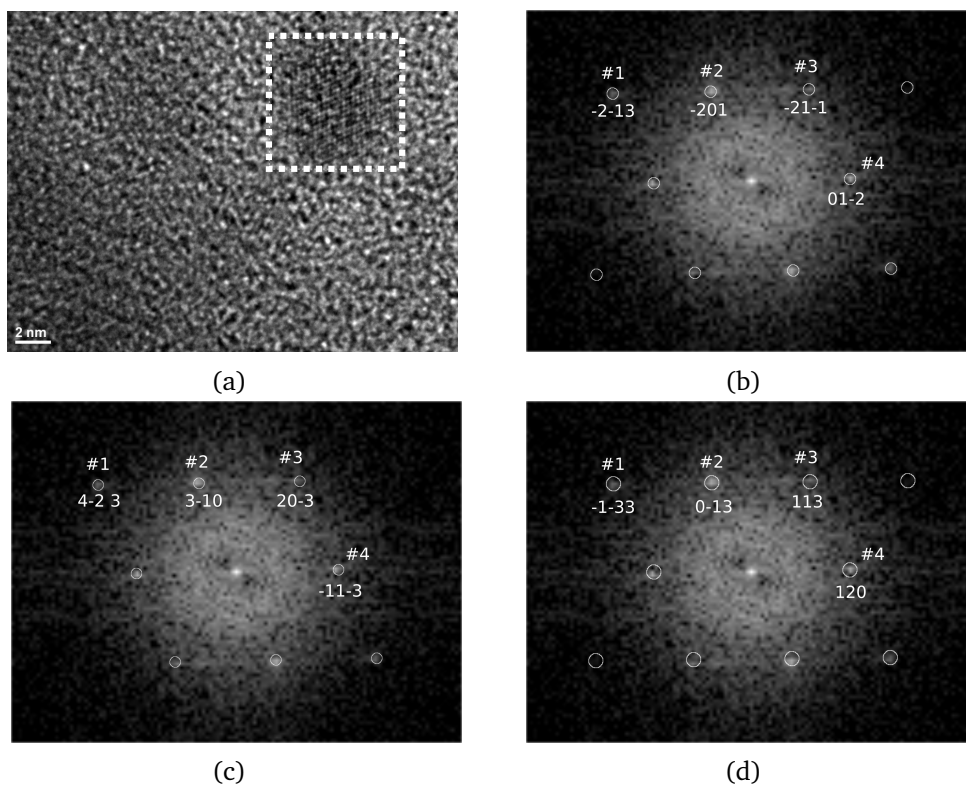


Figure SI3: (a) HRTEM picture of a nanoparticle obtained after decomposition of $\text{Mn}(\text{}^t\text{BuCH}_2)_2$ under 0.9 MPa H_2 at 50 °C for 48 h in $\text{C}_1\text{C}_4\text{ImNTf}_2$. (b), (c) and (d) Corresponding Fourier transform indexed (b) with a β -Mn structure along the (142) direction, (c) with an α -Mn structure along the (-3-9-2) direction, and (d) with a tetragonal structure ($a=6.12 \text{ \AA}$ and $c=9.38 \text{ \AA}$) along the (6-3-1) direction.

3 HRTEM observation of MnO-Cu NPs

The HRTEM image of a nanoparticle obtained after co-decomposition of $\text{Mn}(\text{tBuCH}_2)_2$ and CuMes as well as its Fourier transform are printed in Figure SI4. The latter could be indexed using a tetragonal crystal structure with lattice parameters $a=5.95 \text{ \AA}$ and $c=9.40 \text{ \AA}$ (Figure SI4b and Table SI2).

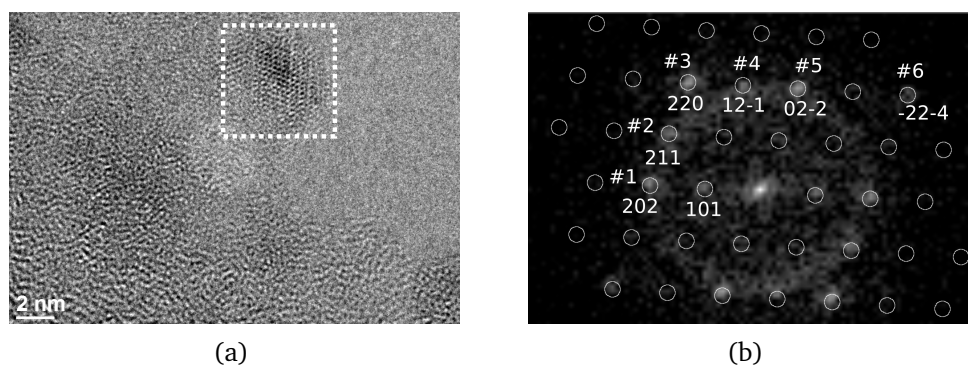


Figure SI4: (a) HRTEM picture of a nanoparticle obtained after decomposition of $\text{Mn}(\text{tBuCH}_2)_2$ and CuMes under 0.9 MPa H_2 at 100°C for 4 h in $\text{C}_1\text{C}_4\text{ImNTf}_2$. (b) Corresponding Fourier transform indexed with a tetragonal structure ($a=5.95 \text{ \AA}$ and $c=9.40 \text{ \AA}$) along the (1-1-1) direction.

Table SI2: Comparison between measured and computed interplanar distances of the NP in Figure SI4.

#	Exp.		Tetragonal	
	\AA		hkl	\AA
1	2.48		202	2.51
2	2.65		211	2.56
3	2.12		220	2.10
4	2.55		12-1	2.56
5	2.54		02-2	2.51
6	1.58		-22-4	1.56

4 XPS and Auger response of Cu in MnO-Cu NPs and deposits

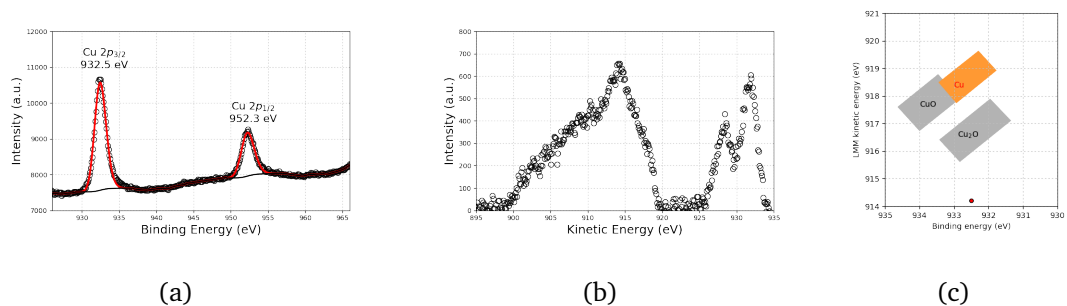


Figure SI5: (a) Cu 2p lines and (b) Cu LMM Auger line measured from a deposit of Cu NPs by XPS and XAES, respectively. (c) Resulting Wagner plot.¹

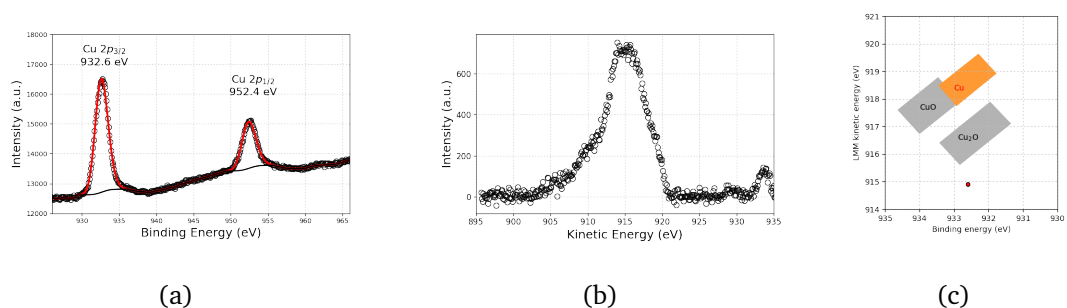


Figure SI6: (a) Cu 2p lines and (b) Cu LMM Auger line measured from a suspension of MnO-Cu-NPs by XPS and XAES, respectively. (c) Resulting Wagner plot.¹

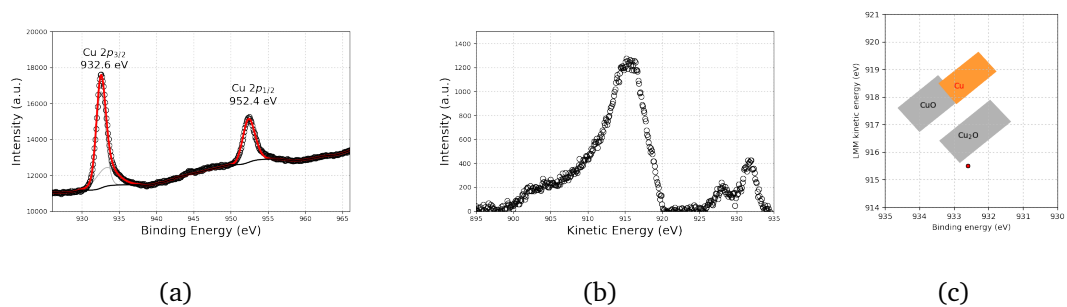


Figure SI7: (a) Cu 2p lines and (b) Cu LMM Auger line measured from a deposit of MnO-Cu NPs by XPS and XAES, respectively. (c) Resulting Wagner plot.¹

5 EDX response of Si substrates coated with MnO, Cu and MnO-Cu NPs

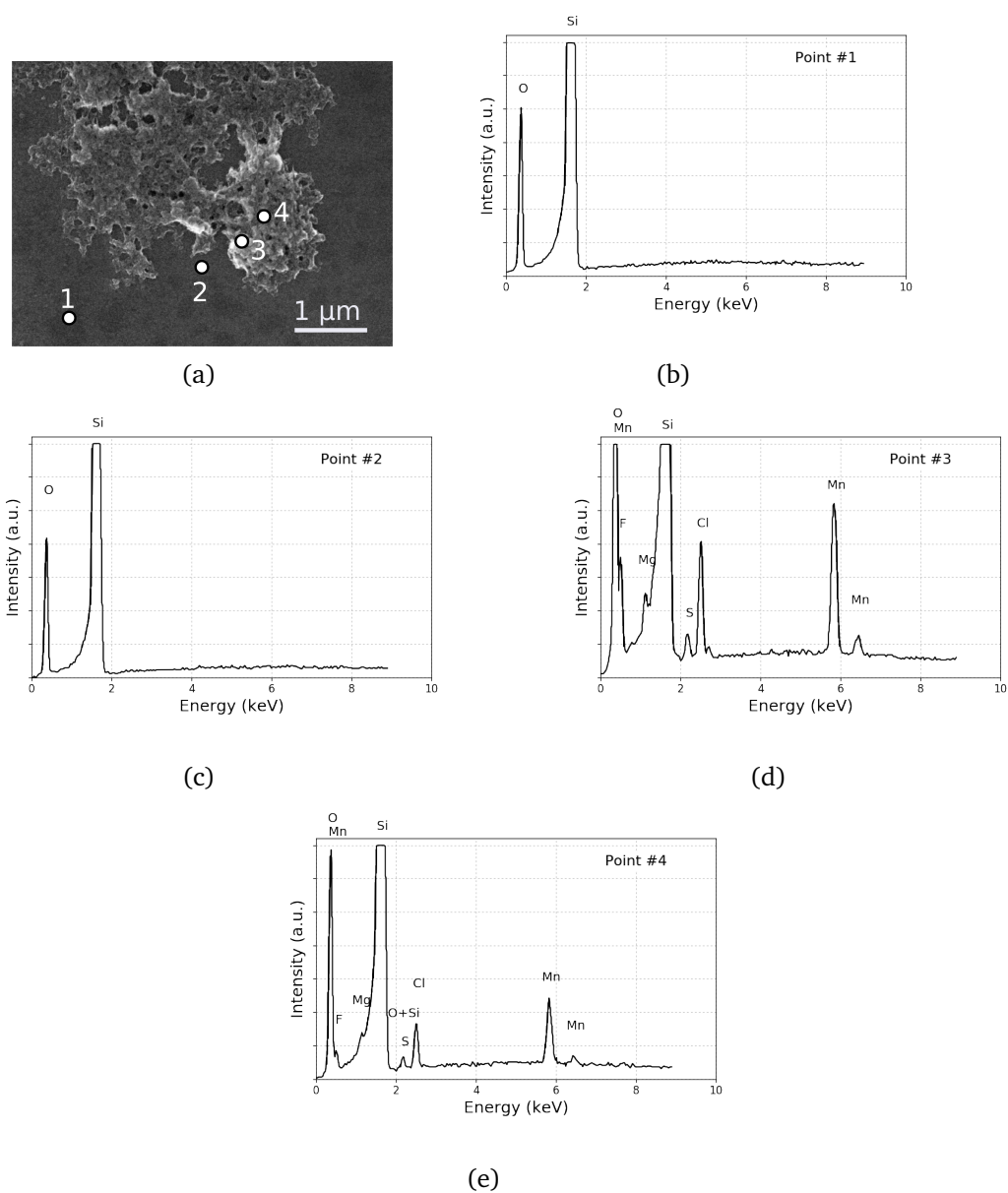


Figure S18: (a) SEM image of a MnO deposit on silica formed by in-situ thermal treatment of a suspension of MnO-NPs in IL at 250 °C for 1 h under N₂/H₂, and (b-e) EDX spectra recorded on the corresponding points of (a).

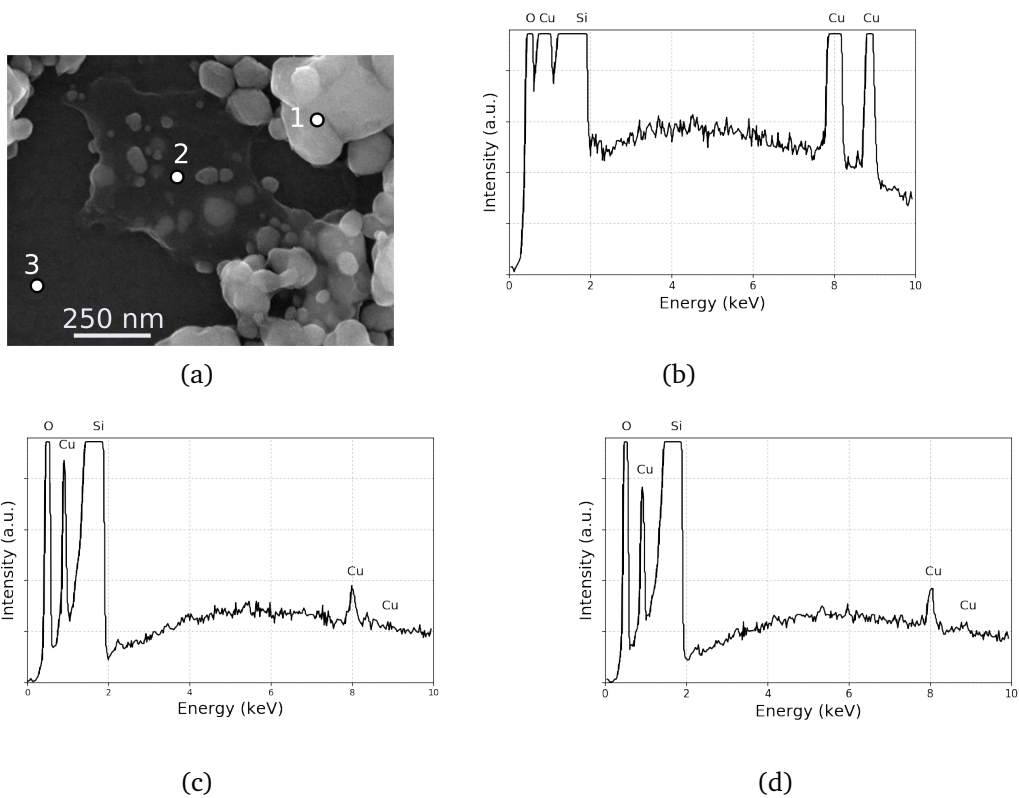


Figure SI9: (a) SEM image of a Cu deposit on silica formed by in-situ thermal treatment of a suspension of Cu-NPs in IL at 250 °C for 1 h under N₂/H₂, and (b-d) EDX spectra recorded on the corresponding points of (a).

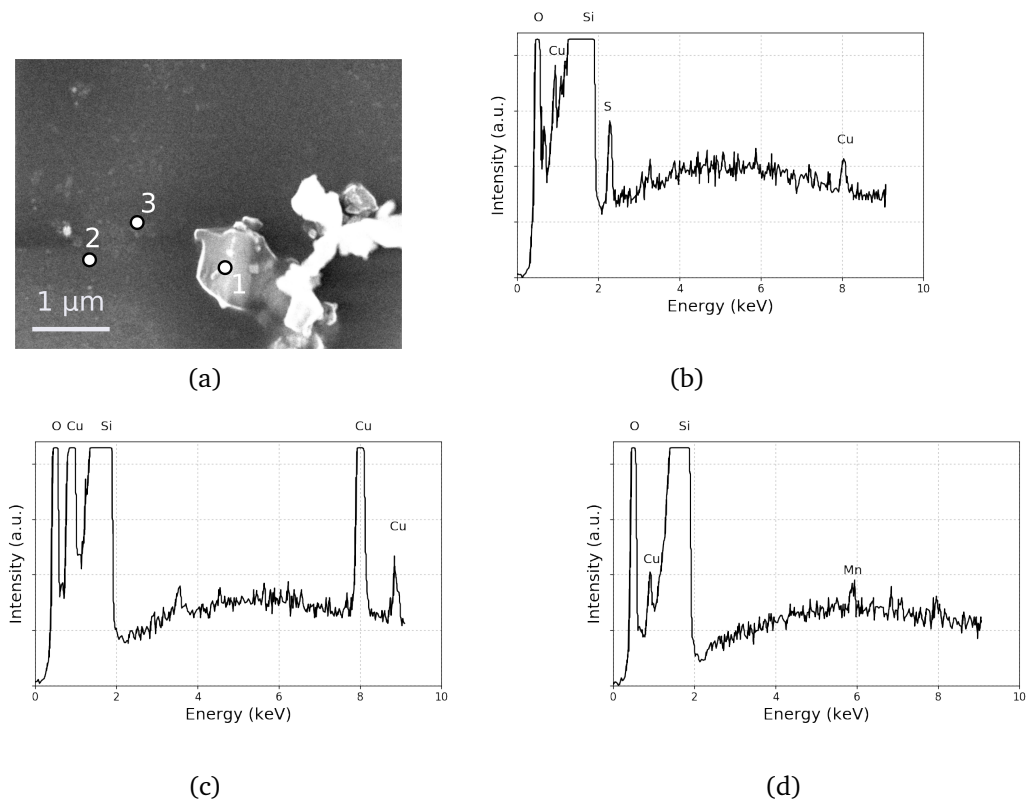


Figure SI10: (a) SEM image of a MnO-Cu deposit on silica formed by in-situ thermal treatment of a suspension of MnO-Cu-NPs in IL at 250 °C for 1 h under N₂/H₂, and (b-d) EDX spectra recorded on the corresponding points of (a).

6 XPS response of Si in substrates coated with MnO, Cu and MnO-Cu NPs

Two components could be resolved from the Si peak from the substrates (Figure SI11). For SiO₂, the only expected contribution is Si(IV) between 103.4 and 103.7 eV.^{2,3} In our samples, an additional peak is detected between 102.1 and 102.3 eV. This contribution is attributed to Si(III)². The ratio between these two contributions was measured for each sample at two locations. The average value for this ratio is reported in Table 1 in the main document.

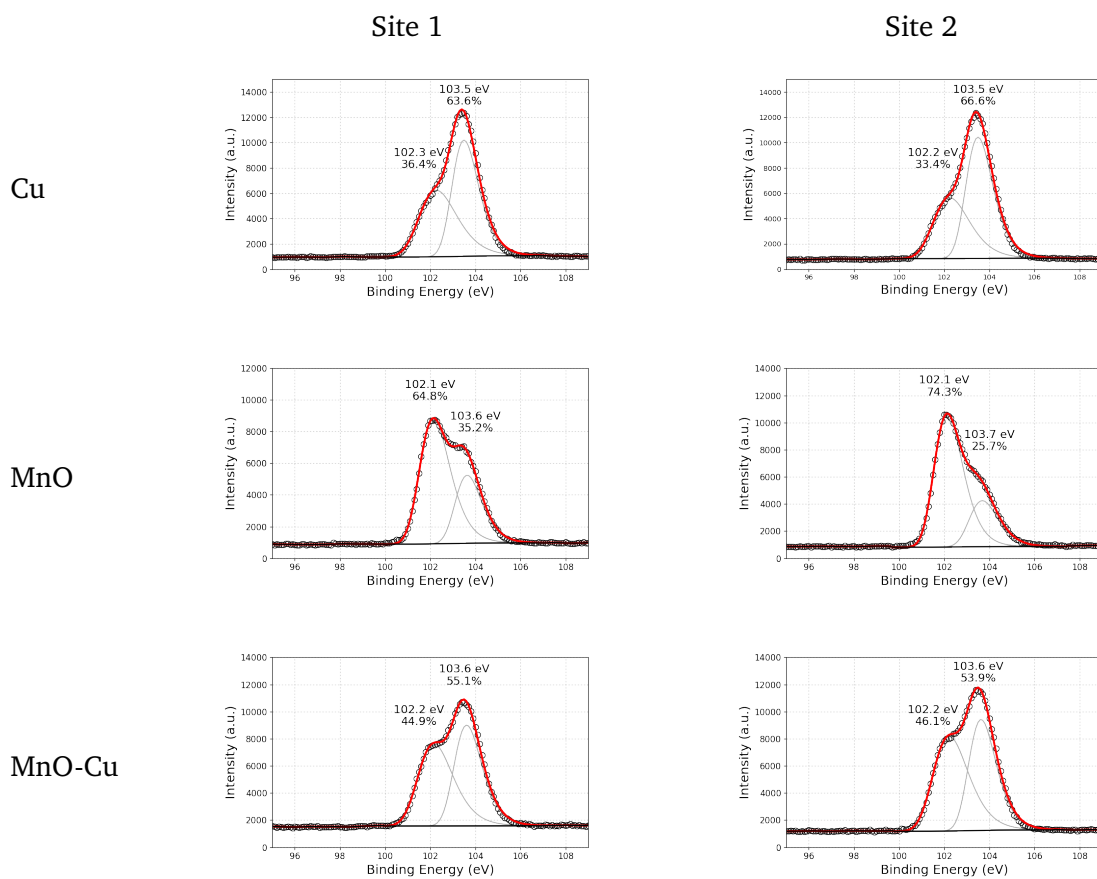


Figure SI11: XPS response of Si at two sites of substrates coated with MnO, Cu and MnO-Cu NPs

References

- [1] C. D. Wagner and A. Joshi, *Journal of Electron Spectroscopy and Related Phenomena*, 1988, **47**, 283–313.
- [2] F. J. Himpsel, F. R. McFeely, A. Taleb-Ibrahimi, J. A. Yarmoff and G. Hollinger, *Physical Review B*, 1988, **38**, 6084–6096.
- [3] R. Sawyer, H. W. Nesbitt and R. A. Secco, *Journal of Non-Crystalline Solids*, 2012, **358**, 290–302.